Biogeosciences Discuss., 11, 2267–2303, 2014
www.biogeosciences-discuss.net/11/2267/2014/
doi:10.5194/bgd-11-2267-2014

Biogeosciences Discussions
Open Access

Consistent increase in dimethyl sulphide (DMS) in response to high CO_2 in five shipboard bioassays from contrasting NW European waters

F. E. Hopkins[1] **and S. D. Archer**[1,*]

[1]Plymouth Marine Laboratory, Plymouth, UK
[*]now at: Bigelow Laboratory for Ocean Sciences, Maine, USA

Received: 31 December 2013 – Accepted: 9 January 2014 – Published: 10 February 2014

Correspondence to: F. E. Hopkins (fhop@pml.ac.uk)

Published by Copernicus Publications on behalf of the European Geosciences Union.

Abstract

The ubiquitous marine trace gas dimethyl sulphide (DMS) comprises the greatest natural source of sulphur to the atmosphere and is a key player in atmospheric chemistry and climate. We explore the short term response of DMS and its algal precursor dimethyl sulphoniopropionate (DMSP) production and cycling to elevated carbon dioxide (CO_2) and ocean acidification (OA) in five highly replicated 96 h shipboard bioassay experiments from contrasting sites in NW European shelf waters. In general, the response to OA throughout this region showed little variation, despite encompassing a range of biological and biogeochemical conditions. We observed consistent and marked increases in DMS concentrations relative to ambient controls, and decreases in DMSP concentrations. Quantification of rates of specific DMSP synthesis by phytoplankton and bacterial DMS gross production/consumption suggest algal processes dominated the CO_2 response, likely due to a physiological response manifested as increases in direct cellular exudation of DMS and/or DMSP lyase enzyme activities. The variables and rates we report increase our understanding of the processes behind the response to OA. This could provide the opportunity to improve upon mesocosm-derived empirical modelling relationships, and move towards a mechanistic approach for predicting future DMS concentrations.

1 Introduction

Dimethyl sulphide (DMS) is a ubiquitous marine trace gas derived from the breakdown of the algal osmolyte β-dimethyl sulphoniopropionate (DMSP). A variety of phytoplankton species produce DMSP, with the majority of production attributed to prymnesiophytes, dinoflagellates and diatoms (Stefels, 2000). Reasons for the algal biosynthesis of DMSP are thought to include a role as an overflow product for the regulation of carbon and sulphur metabolism, as an osmolyte or compatible solute, and/or as a defence mechanism against microbes, viruses and zooplankton grazing. Finally, along with its

BGD
11, 2267–2303, 2014

breakdown products (DMS, acrylate, dimethyl sulfoxide (DMSO)), DMSP scavenges harmful hydroxyl radicals and other reactive oxygen species, potentially providing the cell with anti-oxidant protection (Stefels, 2000; Stefels et al., 2007; Sunda et al., 2002, 2007).

DMSP is released from phytoplankton cells into the dissolved phase by active exudation, or when cells are lysed during grazing, viral attack or senescence (Stefels et al., 2007). Once in this phase, marine bacteria play a vital role in the fate of DMSP in the surface oceans. Indeed, most DMSP released from phytoplankton is either catabolised by bacteria to produce DMS, or demethylated/demethiolated to produce other key organosulphur compounds such as methanethiol (MeSH) (Kiene et al., 2000; Moran et al., 2012). The demethylation/demethiolation (de/de) pathway regularly dominates as it is considered more energetically advantageous than the cleavage pathway (Kiene et al., 2000; Simó et al., 2002; Moran et al., 2012). Thus DMSP turnover often exceeds DMS production in the surface oceans. However, the factors regulating the switch between these two competing pathways are still poorly understood (Moran et al., 2012).

DMS is also subject to rapid biological consumption, a process thought to account for 50–80 % of total DMS loss in the surface oceans, and one which often dominates in bloom situations (Gabric et al., 1999; Simó, 2004). Photochemical loss of DMS competes with this biological loss pathway, comprising a comparable proportion of the total loss (Toole et al., 2006; Vila-Costa et al., 2008). Of the total DMSP produced in the oceans, < 10 % is available for exchange with the atmosphere as DMS –however this flux, amounting to $\sim 28\,\mathrm{TgSyr}^{-1}$, comprises approximately 50 % of the total global natural *S* flux (Andreae, 1990; Kiene and Linn, 2000; Lana et al., 2011). In the atmosphere, DMS is rapidly oxidised forming oxidation products that contribute to the atmospheric aerosol burden, and can lead to the formation and/or growth of particles (Charlson et al., 1987; Barnes et al., 2006). In addition, DMS-derived aerosols are highly effective at influencing cloud albedo, with implications for global radiative forcing (Rap et al., 2013).

BGD
11, 2267–2303, 2014

Increasing atmospheric CO_2 levels and the corresponding oceanic uptake of excess CO_2 is resulting in changes to the carbonate chemistry of the surface oceans. This process, termed ocean acidification (OA), manifests as decreasing carbonate ion concentrations [CO_3^{2-}], increasing hydrogen ion concentrations [H^+] and a corresponding decrease in seawater pH (Caldeira and Wickett, 2003). Since industrialisation, mean surface ocean pH has fallen by 0.1 pH units. A further decrease of 0.4–0.5 pH units by 2100 is likely unless stringent global CO_2 emissions stabilization is implemented (Caldeira and Wickett, 2003, 2005). Such rapid changes to seawater chemistry, potentially unprecedented in the last ~ 300 Ma, are likely to have serious repercussions for marine biological and biogeochemical processes (Raven et al., 2005; Hendriks et al., 2010; Liu et al., 2010; Riebesell and Tortell, 2011; Hönisch et al., 2012).

The majority of OA experiments that consider DMS(P) have been coastal temperate and subpolar mesocosms, with observations of bulk DMS and DMSP made over 3–4 weeks during a nutrient-induced springtime phytoplankton bloom (Wingenter et al., 2007; Vogt et al., 2008; Hopkins et al., 2010; Kim et al., 201, Avgoustidi et al., 2012; Archer et al., 2013). Thus, available data are limited by lack of geographical and seasonal coverage. Decreases in DMS have been observed under predicted turn-of-the-century levels of CO_2, ranging from ~ 35 % (Archer et al., 2013) to ~ 60 % (Hopkins et al., 2010; Avgoustidi et al., 2012) relative to ambient controls. When similar levels of pH-driven changes in DMS concentrations are applied globally, the resultant changes in DMS emissions from the oceans may be sufficiently large to influence climate (Six et al., 2013). However, the pattern of decreasing DMS with decreased pH is not consistent amongst all mesocosm experiments. The study by Kim et al. (2010) reported an ~ 80 % increase in DMS under high CO_2. In one case, little difference in concentrations between ambient and high CO_2 was observed (Vogt et al., 2008). The DMSP response is similarly variable but of comparable orders of magnitude. Simple relationships have been derived with biological measurements (e.g. plankton community structure, pigments, bacterial abundance and rates) as drivers of the observed DMS(P) responses. Physiological effects at the cellular level are more difficult to detect. Broad

BGD
11, 2267–2303, 2014

community-level taxonomic shifts drive the DMS response because the altered conditions favour some species over others (Engel et al., 2008; Meakin and Wyman, 2011; Brussaard et al., 2013). There is still a fundamental lack of mechanistic and physiological understanding of the responses, and limited information on regional variability.

Improved predictive capability of models is likely to require a better understanding of the mechanisms driving OA-induced changes in DMS biogeochemistry. Unialgal cultures potentially provide a useful insight into the specific physiological response of a single species to elevated CO_2. DMS decreased 2- to 10-fold in cultures of the coccolithophore *Emiliania huxleyi* under high CO_2, whereas DMSP responded differently (Arnold et al., 2012; Avgoustidi et al., 2012). Spielmeyer and Pohnert (2012) reported decreases in cellular DMSP in diatoms, but increases in non-calcifying strains of *E. huxleyi*. How informative these results are to the complex DMSP and DMS cycle in natural communities is questionable.

In an attempt to bridge the gap between the complexity of interpreting processes in traditional mesocosm experiments and the limited applicability of unialgal culture experiments to natural systems, this study was designed to assess the short term response of a variety of natural communities from a wide geographic area to high CO_2. Unlike past mesocosm studies, our experiments focus on physiological organism-level acclimation responses in natural communities. By determining rates of key processes, along with standing stock measurements of DMSP and DMS, we can consider a number of hypotheses. Firstly, increased CO_2 may stimulate primary productivity in phytoplankton communities (Riebesell and Tortell, 2011), resulting in enhanced DMSP synthesis rates and increased DMSP concentrations (Archer et al., 2013). Secondly, elevated primary production may stimulate bacterial production by increasing the availability of organic substrates (Weinbauer et al., 2011; Engel et al., 2013; Piontek et al., 2013). This would create a greater bacterial demand for DMSP-sulphur and stimulate the de/de pathway, whilst also resulting in an increase in bacterial DMS consumption. The overall effect would be decreased gross DMS production.

BGD
11, 2267–2303, 2014

2 Materials and methods

2.1 Experimental bioassays

Five shipboard experimental bioassays (hereafter E01–E05) were undertaken during the UK Ocean Acidification research programme (UKOA) NW European shelf cruise aboard the RRS Discovery, 6 June–10 July 2011. Full details of the sampling and experimental setup are given by Richier et al. (2014) and a general overview is given here. For bioassay water collection, a stainless steel CTD rosette comprising twenty-four 20 L bottles was deployed, and all bottles were simultaneously fired at the near surface (5–12 m). Water collection commenced pre-dawn, at 02:00 GMT for E01–E04, and at 01:00 GMT for E05 due to its more northerly location and earlier sunrise time (Locations and sample depths given in Table 1 and Fig. 1). Once the rosette was back on deck, the water was directly transferred into 4 L polycarbonate bottles. Manipulations of the carbonate chemistry were achieved by additions of $NaHCO_3^-$ (1 M) and HCl (1 M) to attain the four target CO_2 levels (ambient, 550 µatm, 750 µatm, 1000 µatm). After first ensuring the absence of bubbles or headspace, the bottles were sealed with septa lids and placed in the incubation container. Bottles were incubated inside a custom designed temperature- and light-controlled shipping container, set to match the in situ water temperature at the time of collection. A constant light level (100 $\mu E\,m^{-2}\,s^{-1}$) incorporating an 18 : 6 light : dark cycle was provided by LED panels. Each bottle belonged to a set of biological triplicates, and sacrificial sampling of bottles was performed at one of two time points (T1: 48 h and T2: 96 h), with three sets of biological triplicates for each time point to allow for the sampling requirements of the entire scientific party (3×3 bottles, $\times 2$ time points, $\times 4$ CO_2 treatments = 72 total). At each time point (48 h and 96 h), the relevant bottles were removed from the incubation container and sampled. Samples for carbonate chemistry measurements were made first to avoid gas exchange with ambient air, followed by sampling for DMS, DMSP and related parameters.

BGD
11, 2267–2303, 2014

2.2 DMS and DMSP standing stocks

The volume of water required to fill all experimental bioassay bottles and to make key initial measurements (carbonate chemistry, nutrients, chl *a*, photophysiology) was such that there was insufficient water for DMS-related initial measurements to be taken from the same CTD cast. Therefore, a second CTD cast was carried out after the bioassay cast to collect additional water for further initial measurements, at the same station and depth, 2–3 h after the primary bioassay cast. It was from these additional CTD casts that all initial DMS and DMSP samples were taken. Samples were taken directly from the Niskin bottles using Tygon tubing, and collected in 250 mL amber glass-stoppered bottles. The bottle was rinsed three times before being filled gently from the bottom, and then allowed to over-flow three times. Once full, the glass stopper was securely placed on the bottle, ensuring the presence of no headspace. Samples were kept in a cool box and analysed within 2 h.

Samples at experimental time points (48 h, 96 h) were taken directly from the bioassay bottles. After inverting the bioassay bottle three times to ensure re-suspension of particulates, samples were siphoned from the bottles using 6 mm silicone tubing directly into 100 mL glass-stoppered bottles. The bottle was first rinsed then filled to the top, ensuring the presence of no bubbles or headspace.

Seawater DMS concentrations were determined by cryogenic purge and trap, followed by detection via gas chromatography with a pulsed flame photometric detector, as outlined in Archer et al. (2013). Total DMSP concentrations (DMSPt) from the same sample bottle were fixed by addition of 35 µL of 50 % H_2SO_4 to 7 mL of seawater (Kiene and Slezak, 2006), and analysed within 2 months of collection, again as described in Archer et al. (2013). DMS calibrations were performed using alkaline cold-hydrolysis (10 M NaOH) of DMSP (> 98 % purity, Centrum voor Analyse, Spectroscopie and Synthese, Rijksuniversiteit Groningen) diluted 3 times in MilliQ water, to give working standards in the range 0.03–3.3 ng S mL^{-1}, and multi-point calibrations were performed every 2–4 days throughout the cruise.

BGD
11, 2267–2303, 2014

2.3 DMSP synthesis and production rates

De novo DMSP synthesis (μ DMSP) and gross production rates were determined for all bioassay experiments at each experimental time point, except for E01. The methods used were similar to Archer et al. (2013), wherein a full and detailed description of the procedures and analyses can be found. For each CO_2 level, triplicate rate measurements were determined. For each rate measurement 3 × 500 mL polycarbonate bottles were filled by gently siphoning water directly from each replicate bioassay bottle. Trace amounts of $NaH^{13}CO_3$, equivalent to ~ 6 % of in situ dissolved inorganic carbon (DIC), were added to each 500 mL bottle. The bottles were incubated in the bioassay incubation container with temperature and light levels as described above. Samples were taken at 0 h, then at two further time points over a 6–9 h period. At each time point, 250 mL was gravity filtered in the dark through a 47 mm GF/F filter, the filter gently folded and placed in a 20 mL serum vial with 10 mL of Milli-Q and one NaOH pellet, and the vial was crimp-sealed. Samples were stored at −20 °C until analysis by proton transfer reaction-mass spectrometer (PTR-MS) (Stefels et al., 2009).

Gross DMSP production rates during the incubations (nmol L^{-1} h^{-1}) were calculated from μDMSP and the initial particulate DMSP (DMSPp) concentration of the incubations. Concentrations of DMSPp were determined at each time point by gravity filtering 7 mL of sample onto a 25 mm GF/F filter and preserving the filter in 7 mL of 35 mM H_2SO_4 in MQ-water. DMSPp concentrations were subsequently measured as DMS following alkaline hydrolysis (see above).

2.4 Biological DMS consumption (BC) and estimation of gross DMS production (GP)

Gross DMS production (GP) by the whole microbial community and bacterial DMS consumption (BC), were determined by dark incubations of whole seawater with ^{13}C-DMS additions. Incubations were performed at each experimental time point of the

BGD
11, 2267–2303, 2014

five bioassay experiments. Six incubations were performed per experiment (i.e. 3 time points for both ambient and 750 µatm CO_2 treatments).

^{13}C-DMS solutions were prepared by reducing ^{13}C-dimethyl sulphoxide (DMSO) (100 µL 99 % DMSO, Sigma Aldrich Co., diluted in 900 µL MilliQ) using sodium borohydride ($NaBH_4$, 1 g left for 5 min). The reactants were purged (20 mL min^{-1} for 20 min) and ^{13}C-DMS collected in a 1/16″ PTFE loop submerged in liquid nitrogen. The ^{13}C-DMS was rinsed into a 20 mL glass serum vial by syringing 15 mL of MilliQ through the sample loop. The serum vial was crimp sealed and stored in the dark at 4 °C. The primary solution underwent two serial dilutions in MilliQ to produce a working solution.

For each incubation, 500 mL of seawater was siphoned from the bioassay bottle into an acid-washed (1 % HCl) and thoroughly rinsed 1 L Tedlar bag. Once filling was complete, any bubbles and headspace were gently expelled from the bag. Each bag was spiked with small volumes (100–150 µL) of a working solution of ^{13}C-DMS (in MilliQ water) to give concentrations of 0.1–0.3 nM. After spiking, the bags were left for one hour to allow complete homogenisation of the tracer. Bags were incubated in the dark, and concentrations of ^{13}C-DMS and ^{12}C-DMS were monitored to determine ^{13}C-DMS loss rates, and net and gross DMS. Sub-samples (20 mL) were withdrawn using a glass syringe at 0 h and at 3 further time-points over a 10–12 h period. The samples were gently filtered through a Millipore filtration unit containing a 25 mm GF/F filter, directly into a 10 mL glass syringe and 8 mL of filtered seawater was injected into a glass purge tower. The addition of air and bubbles was avoided or minimised at all times. The sample was purged for 8 min at 90 mL min^{-1}, dried with a PTFE counterflow nafion drier, and trapped in a 1/16″ PTFE loop held in liquid nitrogen. Once purging was complete, the sample loop was rapidly submerged in boiling water, injecting the sample into an Agilent 5973N gas chromatograph with a 60 m DB-VRX capillary column and mass spectral detector (MSD). The oven was held at 60 °C for 8 min, and ramped to 220 °C for the remainder of the 10 min runtime. DMS and ^{13}C-DMS eluted from the column at ~ 5.3 min. To monitor system sensitivity and drift, 100 µL of a 5 ppmv deuterated DMS (CD_3SCD_3) gas standard was injected upstream of each sample. The MSD was oper-

BGD
11, 2267–2303, 2014

ated in single ion mode (SIM) and was programmed to detect the following ions: m/z 62, 61 and 47 for ^{12}C-DMS, m/z 64 for ^{13}C-DMS, and m/z 68 for CD_3SCD.

Calibrations were performed using pure DMS (> 99 %, Sigma Aldrich Co.) diluted in MilliQ water. A primary standard was gravimetrically prepared, and then serial dilutions were performed to obtain a working standard of 0.3 ng S mL^{-1}. Multi-point calibrations, from 0 to 3.5 ng S mL^{-1}, were performed every 3 days for the duration of the cruise. Detection limits for ^{12}C-DMS and ^{13}C-DMS were 0.1 ng S and 0.03 ng S, respectively. The lower detection limit for ^{13}C-DMS is the result of lower background concentrations of this isotope in blank measurements. Average analytical precision based on triplicate samples was ~ 10 %.

Rates of BC (nmol L^{-1} d^{-1}) were estimated from the slope of the linear decrease in ^{13}C-DMS concentrations over the 10–12 h incubation period. DMS loss via photochemistry and gas exchange was excluded, so the ^{13}C-DMS loss is considered to be equivalent to biological consumption. To scale to in situ DMS concentrations, BC rates were first divided by the concentration of ^{13}C-DMS tracer (giving first order rate constants, d^{-1}), and multiplied by in situ DMS concentrations. The ^{12}C-DMS change during the incubations represents the net DMS production rate. The GP was estimated as the difference between net DMS production and BC.

Additions of ^{13}C-DMS ranged from 10–100 % of ambient DMS concentrations. Large relative additions of ^{13}C-DMS were unavoidable when ambient DMS concentrations were low (< 1 nmol L^{-1}) due to the limits of detection of the method. The following equation was used to correct BC rates for any enhancement caused by tracer addition ($rDMS_t$, Rees et al., 1999), which was originally described for the correction of ^{15}N ammonium uptake rates:

$$rDMS_t = \frac{rDMS_o}{DMS_{tot}/(Ks + DMS_{tot}) \cdot (Ks + DMS_a)/DMS_a} \quad (1)$$

where $rDMS_t$ = loss rate adjusted for stimulation by tracer (nmol L^{-1} d^{-1}), $rDMS_o$ = original loss rate (nmol L^{-1} d^{-1}), DMS_{tot} = [DMS] ambient + [^{13}C-DMS]

BGD
11, 2267–2303, 2014

(nmol L^{-1}), DMS_a = [DMS] ambient (nmol L^{-1}), and Ks = half saturation parameter (nmol L^{-1}). The value of Ks was taken as the mean of the Ks determined through three kinetic experiments described in the Supplement.

2.5 Total bacteria abundance

Samples for determination of total bacteria abundance were taken in triplicate at the start of all incubations for BC/GP. 20 uL of glutaraldehyde solution (Grade 1, 50 % in H_2O, Sigma Aldrich Co.) was added to 2 mL samples, and the vials were fixed for 30 min at 4 °C, followed by snap freezing in liquid nitrogen and storage at −80 °C until analysis. Bacteria were counted by flow cytometry according to Marie et al. (1999). Briefly, thawed samples were diluted with Tris-EDTA buffer (10 mM Tris-HCl and 1 mM EDTA, pH 8) and stained with the green fluorescent nucleic acid-specific dye SYBR-Green I (Molecular Probes, Invitrogen Inc.) at a final concentration of 1×10^{-4} of the commercial stock, in the dark at room temperature for 15 min. Bacteria were discriminated in bivariate scatter plots of green fluorescence vs. side scatter.

3 Results

3.1 Experimental bioassays: starting conditions

The design of this study allowed an assessment of the response of surface ocean communities to high CO_2 during the most biologically productive time of year by sampling a variety of seasonally stratified (E01, E03, E05) and perennially mixed (E02, E04) sites, both on- and off-shelf (Fig. 1). Initial conditions generally displayed typical NW European shelf summertime characteristics, with low concentrations of nutrients (< 1.1 µM total organic nitrogen (TON), ~ 0.1 µM P), and a range of chl *a* concentrations (0.8–3.3 µg L^{-1}) reflecting the heterogeneous spatial distribution of marine productivity in shelf sea waters. In situ pCO_2 concentrations were similarly variable, ranging from

BGD
11, 2267–2303, 2014

334 µatm for E02 to 401 µatm for E04 (see Table 1). Further detail is given elsewhere (Richier et al., 2014).

3.2 DMSPt and DMS: concentrations and ratios

Triplicate bottles displayed highly repeatable values and trends of DMSPt over the course of all experiments. Initial concentrations in the five bioassays spanned a wide range, from 8.0 nmol L^{-1} for E04 to 59.6 nmol L^{-1} for E01 (Table 1). There was a net increase in DMSPt for all ambient control incubations after 96 h, with the greatest increase seen over the first 48 h. For all experiments, a clear response to increasing levels of CO_2 was observed (Fig. 2a–e), with a large number of significant reductions in DMSPt with increasing CO_2 concentrations after 48 h (ANOVA, Holm-Sidak, $P < 0.05$, Table S2). After 96 h, concentrations showed some recovery in high CO_2 treatments for E02 and E04, but the response persisted for E01, E03 and E05. In addition, when all data was included in a single analysis a significant negative relationship between DMSPt and $[H^+]$ data was seen (ANOVA, significance of F ratio $P < 0.001$, Table S3).

Again, concentrations and trends of DMS from triplicate bottles were highly repeatable for all experiments. Initial mean concentrations of DMS (Fig. 2f–j) varied by a factor of three, from 0.7 nmol L^{-1} (E02) to 2.1 nmol L^{-1} (E03), and higher DMS concentrations tended to be associated with lower chl *a* (Table 1). Net DMS accumulation was observed in all ambient control incubations over 96 h. There was a clear response to high CO_2 in all experiments, with significantly elevated DMS concentrations, predominantly after 48 h (ANOVA, Holm-Sidak, $P < 0.05$, Table S2). The response became more variable after 96 h, with rapid rises in DMS in ambient controls for E01, E03 and E04, resulting in concentrations similar to those under high CO_2. For all experiments at each time point (with the exception of E04 at 96 h) significant positive relationships between DMS concentrations and $[H^+]$ were observed (Table S3). The relationship between these variables was strongest at 48 h (r^2 = 58.4–91.5, $P < 0.01$), and generally weakened at 96 h (r^2 = 34.9–79.3, $P < 0.05$).

BGD
11, 2267–2303, 2014

In summary, large increases in mean DMS concentrations relative to ambient controls were observed in all bioassays: 110 % (28–223 %) at 550 µatm, 153 % (56–295 %) at 750 µatm and 225 % (79–413 %) at 1000 µatm. By contrast, mean DMSPt concentrations showed a consistent decrease, but to a lesser extent than DMS: 28 % (18–40 %) at 550 µatm, 44 % (18–64 %) at 750 µatm and 52 % (24–72 %) at 1000 µatm.

Initial DMS : *DMSPt* ratios ranged from 0.02 for E01 to 0.14 for E04 (Fig. S3). This ratio gradually increased over 96 h (except in E04), and for all experiments was significantly correlated with increasing [H^+] after both 48 h and 96 h (Fig. 3 and Table S3, ANOVA of regression, F ratio $P < 0.05$). DMS : chl *a* ratios generally followed similar trends to DMS : *DMSPt* (Fig. S3). Significant positive relationships between DMS : chl *a* and [H^+] were identified for all experiments at 48 h (ANOVA of regression, F ratio $P < 0.001$, except E04 $P < 0.05$, Table S3). By 96 h, this relationship remained significant for all experiments, but was negative for E01 and E04.

DMSPt : chl *a* also showed large variation between experiments, from < 30 nmol µg^{-1} in E02 up to ~ 150 nmol µg^{-1} in E03 (Fig. S3). In general, increasing [H^+] was associated with a decrease in *DMSPt* : chl *a* but this relationship was found to be significant only for E01 and E04 at 48 h. By 96 h, the majority of experiments displayed a significant negative relationship between these variables (ANOVA of regression, F ratio $P < 0.01$, Table S3).

3.3 Plankton community and OA response

In general, an increase in abundance of small phytoplankton (< 10 µm, pico- and nanophytoplankton) was seen over the experimental period, indicating growth within the bioassay bottles (Fig. 2k–o). For E02–E05, abundances were significantly lower under high CO_2 at both 48 h and 96 h (ANOVA, Holm-Sidak, $P < 0.05$, Table S4). By contrast, there were significant increases in abundance under high CO_2 (750 and 1000 µatm) at 96 h for E01 (ANOVA, Holm-Sidak, $P < 0.001$, Table S4). The reader is directed to Richier et al. (2014) for further description of the response of small phytoplankton.

BGD
11, 2267–2303, 2014

3.4 DMSP synthesis and production

Initial DMSP synthesis rates (μDMSP) ranged from 0.33 d^{-1} in E05 to 0.96 d^{-1} in E03. Rates tended to decrease over the course of 96 h to ~ 0.10–0.50 d^{-1} (Fig. 4a–d). The effect of CO_2 treatment on μDMSP was variable. Marked decreases in μDMSP at high CO_2 relative to ambient controls were seen for E02 at 48 h (55–65 % decrease) and 96 h (66–74 % decrease), and for E05 at 48 h (42–90 % decrease). For E03 and E04, μDMSP in high CO_2 treatments were generally indistinguishable from ambient controls.

Temporal trends in DMSP production rates corresponded closely with those for μDMSP (Fig. 4e–h). Thus variations in production rates are generally a reflection of physiological alterations in the specific synthesis rates of DMSP, rather than a reflection of taxonomic changes that may influence DMSP production. Initial DMSP production rates ranged from 7.1 nmol L^{-1} d^{-1} in E05 to 37.3 nmol L^{-1} d^{-1} in E03. For E02 and E05, clear decreases in DMSP production rates were observed in the high CO_2 treatments. In E02, this difference was maintained for the duration of the experiment with a mean of 12.0 nmol L^{-1} d^{-1} at ambient CO_2, compared to 1.8–3.1 nmol L^{-1} d^{-1} at elevated CO_2. Similarly large decreases in mean DMSP production were seen in E05 (2.9–11.1 nmol L^{-1} d^{-1} high CO_2, 13.4 nmol L^{-1} d^{-1} ambient CO_2). Similarly to μDMSP, there were no clear differences between treatments for E03 and E04.

3.5 Bacterially-mediated DMS processes

3.5.1 Total bacteria abundance

Initial abundances of bacteria (Fig. 5a–e) in the sub-incubations for BC and GP rates were statistically similar (Kruskal–Wallis $H = 3.273$, $df = 3$, $P = 0.415$), ranging from 0.83 (±0.01) to 1.00 (±0.16) $\times 10^6$ cells mL^{-1} (no data available for E01 0 h). For E01, E02, E04 and E05 bacterial abundance increased with increasing CO_2. Small differences in abundance at 48 h were followed by large increases in bacteria at 750 μatm

BGD
11, 2267–2303, 2014

by 96 h. By contrast, a decrease in bacterial abundance in response to increased CO_2 was observed for E03.

3.5.2 Biological DMS consumption (BC)

Rates of biological DMS consumption (BC) across the five bioassay experiments ranged from 0.2 ± 0.1 to 8.6 ± 1.6 nmol L^{-1} d^{-1}, with the highest overall mean values observed during E01 at Mingulay Reef (3.6 ± 0.7 nmol L^{-1} d^{-1}), and the lowest during E02 in the Irish Sea (0.5 nmol L^{-1} d^{-1}) (see Fig. 5f–j and Table S5). All rates fell well within the range of a variety of previous studies (0.02–8.8 nmol L^{-1} d^{-1}, Bailey et al., 2008; Kiene et al., 2007; Toole and Siegel, 2004; Toole et al., 2006; del Valle et al., 2009; Vila-Costa et al., 2008; Zubkov et al., 2002, 2004). Overall, no clear consistencies in the response of BC to CO_2 treatment were observed. For E01 and E02, BC was greater at high CO_2, with significant differences after 48 h (ANOVA F ratio $P < 0.05$). For E03, BC was lower under high CO_2, although the differences were not significant. For E04 and E05, significant decreases in BC after 96 h were observed (ANOVA F ratio $P < 0.05$).

3.5.3 Biological DMS turnover

DMS turnover time due to biological consumption (τ_{BC}, d), calculated as the inverse of the loss rate constant (k_{BC},d^{-1}) (Fig. 5k–o and Table S5), ranged from < 1 d (E01, E05) to a maximum of 12.3 d (E02). Similarly to BC, there was a lack of consistent response to high CO_2. For experiments E03–E05, turnover over times were consistently higher at high CO_2, but the differences were only significant for E03 (48 h) and E04 (96 h).

3.5.4 Gross DMS production (GP)

Mean gross production rates of DMS (GP) in the five bioassay experiments ranged from undetectable levels during E02, up to a maximum of 8.7 ± 1.4 nmol L^{-1} d^{-1} during E05 (Fig. 5p–t, Table S5). The negative value observed at 48 h in the ambient treatment for

BGD
11, 2267–2303, 2014

E02 was not significantly different from zero, so GP was considered to be undetectable in this case. Overall, a response of GP to high CO_2 was variable or undetectable. GP was significantly elevated at high CO_2 for E02 at 96 h and E03 after 48 h, whilst a significant decrease in GP was observed for E04 at 96 h (ANOVA F ratio $P < 0.05$). No significant differences were seen for E01, E04 and E05.

4 Discussion

Despite variability in physical, biological and biogeochemical characteristics of sampling stations, experimental bioassays gave highly consistent and reproducible DMS(P) responses to OA, affirming the strength of the experimental approach adopted here. Large increases in mean DMS concentrations relative to ambient CO_2 controls were observed in all bioassays: 110 % (28–223 %) at 550 µatm, 153 % (56–295 %) at 750 µatm and 225 % (79–413 %) at 1000 µatm. By contrast, mean DMSPt concentrations showed a consistent decrease: 28 % (18–40 %) at 550 µatm, 44 % (18–64 %) at 750 µatm and 52 % (24–72 %) at 1000 µatm. Our results are in opposition to the majority of results from mesocosm studies. We examine the possible drivers of the observed responses in the following section.

4.1 Influence of plankton community response on DMS(P)

Primarily as a result of the characteristic community dynamics of mesocosm experiments, our current knowledge of the algal physiological effects of OA on the production of DMSP and DMS is minimal. Archer et al. (2013) were the first to determine rates of DMSP synthesis and production during a mesocosm experiment in Svalbard. Increasing CO_2 resulted in elevated gross primary productivity, partly accounted for by an increase in net production of the dinoflagellate *Heterocapsa rotundata*. As DMSP synthesis is tightly coupled to cell metabolism (Stefels, 2000), the increased production in *H. rotundata* was associated with an increase in DMSP production rates and stand-

BGD
11, 2267–2303, 2014

ing stocks. Thus, by focussing in on short term physiological processes relevant to the bioassay experiments, this suggests that increased CO_2 will drive increases in primary production, resulting in enhanced DMSP production rates.

Despite observations of a stimulating effect of CO_2 on photosynthesis and carbon fixation in a range of phytoplankton taxa and natural assemblages (Riebesell and Tortell, 2011), there was no evidence for enhanced productivity during the bioassay experiments. Primary production data for E02 and E03 showed a tendency to decrease under high CO_2 (A. Poulton, personal communication, 2013). In all experiments, except E01, the abundance of small phytoplankton (< 10 µm) was significantly lower under high CO_2 (Fig. 2k–o, Table S4). For E03, E04 and E05, significantly lower [chl *a*] with increasing CO_2 was also observed (see Richier et al., 2014). As a result of this general reduction in phytoplankton biomass and productivity, ratios of *DMSPt* : chl *a* were predominantly lower under high CO_2 (Fig. S3). Furthermore, specific rates of DMSP synthesis (µDMSP) and DMSP production rates were either insensitive to high CO_2 (E03, E04) or showed marked declines (E02, E05) (Fig. 4a–d), likely a simple reflection of a general decline in biological productivity.

Importantly, this general decrease in growth of small phytoplankton coincided with significant increases in DMS : *DMSPt*, suggesting a relationship between these two responses. OA results in a reduction in buffer capacity that may affect proton concentration ($[H^+]$) and/or regulation at the cell membrane surface of phytoplankton. Larger cells (> 25 µm) possess thicker boundary layers and under present day conditions experience such changes over the course of a diel cycle (Flynn et al., 2012). As such, they are better adapted than smaller cells (< 25 µm) to the higher $[H^+]$ that may be encountered under future OA. During the experimental bioassays, rapid changes to seawater chemistry may have induced changes to external cell surface $[H^+]$ beyond that experienced by small cells in the present day oceans, resulting in deleterious effects on the growth of this fraction of the population. This is evidenced by reduced growth of small phytoplankton (< 10 µm) under high CO_2 in most experiments, summarised here in Fig. 2k–o and Table S4 and discussed further by Richier et al. (2014).

BGD
11, 2267–2303, 2014

Gali et al. (2013) proposed that exposure to sub-lethal or lethal levels of ultra-violet radiation (UVR) could induce an increase in cell membrane permeability, eventually triggering apoptosis. This would lead to the release of intracellular DMSP, increasing its availability for catabolism by bacteria, and/or extracellular DLA. In the bioassays, DMSPt concentrations fell and DMS production was stimulated, suggesting a similar mechanism played a role. Small phytoplankton can contribute between 40 % and 57 % to the total DMSP pool (Archer et al., 2011), and thus possess a large potential for DMS production. However, rather than radiation-induced damage, sublethal/lethal cellular damage to small phytoplankton cells induced by rising $[H^+]$ may have resulted in the strong increase in DMS : *DMSPt* ratio. However, the same response was seen in E01 despite an increase in abundance of small phytoplankton cells with increasing CO_2 (Fig. 2k).

Uniquely, E01 at Mingulay Reef was dominated by small cryptophytes ($\sim 10\,\mu m$), whereas all others comprised a mainly $< 10\,\mu m$-sized community. Despite a similar overall response in DMS standing stocks, differences in initial community structure could result in a different cellular mechanistic response to increased CO_2. Rather than cells releasing DMSP/DMS as described above, a physiologically-mediated overflow mechanism could have played a role. The cellular release of DMS is thought to facilitate the removal of surplus sulphur, carbon and energy, allowing the cell to continue functioning during periods of cellular stress or unbalanced growth (Stefels, 2000). This process depends on a direct up-regulation of the conversion of DMSP to DMS via DMSP lyase activity (DLA). Previous studies have demonstrated up to an order of magnitude increase in DMS production in phytoplankton exposed to UV stress (Sunda et al., 2002; Archer et al., 2010). The observed increases of DMS : *DMSPt* with increasing CO_2 may be a manifestation of such a response. Such a process could, to some extent, be relevant to the results of all bioassay experiments.

BGD
11, 2267–2303, 2014

4.2 Influence of bacterial community response on DMS(P)

Previous OA studies suggest increased primary production and photosynthesis at high CO_2 may stimulate bacterial production by increasing the availability of organic substrates for bacterial utilisation (Weinbauer et al., 2011; Engel et al., 2013; Piontek et al., 2013). Such conditions could generate a greater bacterial demand for DMSP-sulphur, leading to an increase in bacterial DMSP catabolism via the de/de pathway, and reductions in gross DMS production (Kiene et al., 2000). This mechanism could explain some of the reduction in DMS concentrations under high CO_2 seen during mesocosm studies (Hopkins et al., 2010; Avgoustidi et al., 2012; Archer et al., 2013). These previous findings suggest increased CO_2 may stimulate bacterial production, and (i) increase bacterial DMSP demethylation/demethiolation (de/de) and/or (ii) increase bacterial DMS consumption resulting in reduced gross DMS production, resulting in reduced gross DMS production.

However, there were few instances of significantly elevated dark DMS gross production rates in response to high CO_2 (Fig. 5 and Table S5). For some experiments (E02, E03 and E04), trends in GP rates were comparable to temporal trends in net concentrations from the bioassays suggesting microbial DMS production is an important contributor to total DMS production, particularly in the latter stages of the bioassays (>48 h). However, it seems unlikely that the rapid increases in DMS yield seen in the first 48 h can be fully explained by an increase in bacterial DMS production.

We also examined the response of biological consumption (BC) of DMS to elevated CO_2, a process thought to account for 50–80 % of total DMS loss in the surface oceans (Gabric et al., 1999; Simó, 2004). Increased bacterial production at high CO_2 may lead to increased bacterial consumption of DMS, resulting in a decrease in gross DMS production. Rates of BC during this study ranged from 0.2–8.6 nmol L^{-1} d^{-1} falling well within the range of previous studies (0.02–8.8 nmol L^{-1} d^{-1}, Bailey et al., 2008; Kiene et al., 2007; Toole et al., 2004, 2006; del Valle et al., 2009; Vila-Costa et al., 2008; Zubkov et al., 2002, 2004). Similarly, turnover times ranged from 0.2–12.3 d, again

BGD
11, 2267–2303, 2014

similar to earlier studies (0.7–18.7 d). The wide range in rates seen here reflects the highly heterogeneous spatial variability of both biomass and surface seawater DMS in NW European shelf waters during summertime. In addition, the results from three kinetic experiments revealed a large range in values of Ks and Vmax in the study waters, implying contrasting levels of control of BC on surface ocean DMS concentrations in the study region (see supplementary information, Table S5). The three sites (KE1, KE2 and KE3) encompassed a wide range of surface DMS concentrations of 1.0, 3.8 and 16.8 nmol L^{-1}, respectively, and this was likely a reflection of the contrasting BC characteristics of the sites (Fig. S1).Vmax ranged from 1.3 to 25.9 nmol L^{-1} d^{-1}. Ks was inversely proportional to in situ DMS, demonstrating the saturation of BC at higher concentrations. For KE3, BC appeared to be close to saturation, suggesting a slow response of DMS consumers to rapidly increasing DMS concentrations at this site, reflected in low Ks of 4.5 nmol L^{-1} and long turnover time of ~ 13 d (Table S5). Such large accumulations of DMS concentrations occur during the breakdown of phytoplankton blooms dominated by DMSP-producers and have previously been attributed to low saturation kinetics of DMS consumers (Wolfe et al., 1999; Simó et al., 2000). Where DMS concentrations were lower for KE1 and KE2, Ks attained greater values of 11–25 nmol L^{-1} and rapid turnover times of ~ 0.1 d were observed. Clearly, at these sites DMS consumers were able to exert a strong control over the accumulation of seawater DMS.

In the context of the bioassays, DMS concentrations generally did not exceed 9 nmol L^{-1}, apart from in two cases where concentrations of > 10 nmol L^{-1} were measured at 1000 µatm in E01 and E03 (Fig. 2f and h). With Ks in the range 4.5–25.0 nmol L^{-1}, it was unlikely that this process was saturated during the bioassays, allowing consumption to continue unabated despite rapid rises in DMS concentrations. In the two cases where DMS did exceed 10 nmol L^{-1}, it is possible that saturation of consumption kinetics was exceeded. However, this was likely a result of, rather than cause of, the DMS CO_2 response. With this is mind, were the observed increases in DMS concentrations driven by CO_2-driven reductions in BC? Although variations in

BGD
11, 2267–2303, 2014

BC between ambient and 750 µatm were observed (Fig. 5f–j, Table S5), the observed differences were not consistent enough to explain the changes in bulk DMS concentrations. Thus bacterial consumption of DMS in the bioassays was not sensitive to increasing CO_2 concentrations.

4.3 Exploring the regional variability

Despite this study targeting sites with a range of physical, biological and biogeochemical characteristics, the overall response to high CO_2 was remarkably consistent, suggesting limited regional variability. In Fig. 7, DMSPt and DMS concentrations under high CO_2 are normalised to those in ambient controls to allow comparison of the relative changes seen for each experiment. The general response is clear; however analysis of variance reveals some significant differences in the extent of the response at each station, suggesting varying levels of resilience in the communities.

The relative decreases in DMSPt concentrations were broadly consistent, ranging from 10 to 30 % relative to controls – except E05 with a mean decrease of ∼ 50 % (Fig. 6a). However, the relative increases in DMS were more variable between stations, from only ∼ 10 % for E04 up to ∼ 190 % for E01 (though accompanied by the greatest range) (Fig. 6b). Such variability is not surprising given the complex nature of DMSP and DMS seawater dynamics. Furthermore, the extent of the response to high CO_2 may be a reflection of the potential community DMS yield. Is it possible to attribute this variability to differences in the characteristics of each station? To simplify the discussion and explore this hypothesis further, we will focus on E01 and E04 as representative of each end of the DMS response spectrum.

Unsurprisingly, E01 and E04 showed differences in phytoplankton biomass, abundance, and speciation (see Richier et al., 2014), which will exert an influence on DMS yields. Initial chl *a* concentrations were 2.5-fold higher at E01 compared to E04 (see Table 1), accompanied by a ∼ 5-fold greater abundance of the > 10 µm size-class (654 cells mL^{-1} compared to 134 cells mL^{-1}, see Richier et al., 2014). This size-class heavily dominated the total phytoplankton biomass at E01, and was mainly comprised

BGD
11, 2267–2303, 2014

of cryptophytes (~ 75 % of > 10 µm fraction, Richier et al., 2014) – though a group not considered to be major DMSP producers (Archer et al., 2011). By contrast, the majority (75–80 %) of chl *a* at E04 was accounted for by the < 10 µm size-fraction of the community, a group which may contribute a large proportion of DMSP to the total seawater pool (Archer et al., 2011). The response of the < 10 µm phytoplankton differed between the two stations, with suppressed growth under high CO_2 for E04 typical of all other experiments, as opposed to increases in abundance for E01 (Fig. 2k and n). As discussed in the previous section, size-related differences in community structure (< 10 µm E04 vs. > 10 µm E01) and differing responses/resiliencies of phytoplankton species (lethal cellular damage vs. physiological mechanisms) are likely to have contributed to the differences in sensitivity to increasing CO_2 between the two stations.

Further insight may be gained by considering the influence of microbial community processes on the observed differences between the two stations. We observed large differences in gross DMS production rates (dark) between E01 and E04 (Fig. 5, 2–6 nmol L^{-1} d^{-1} compared to 0.5–2 nmol L^{-1} d^{-1}, respectively), indicating that the community at E01 had greater potential DMS yield. By contrast, DMS consumption (dark) was within a similar range for both experiments (Fig. 5), and perhaps unimportant in determining the community DMS yield at these stations. Thus at E04, relatively large mean decreases in DMSPt were not translated to similar mean increases in DMS (Fig. 6). Supported by low gross DMS production rates (Fig. 5s), this suggests that bacterial catabolism via the de/de pathway may dominate DMSP cycling at this station. At E01, a similar relative decrease in DMSPt resulted in a much greater DMS yield, accompanied by relatively high gross DMS production rates (Fig. 5p). Thus, bacterial DMSP cleavage may be more important here.

Water column structure and exposure to solar irradiance are thought to be important factors in determining the DMS yield of a community (Simó and Pedrós-Alió, 1999; Toole et al., 2003, 2006; Toole and Siegel, 2004; Vallina and Simó 2007; Miles et al., 2012). For example, a shallow mixed layer depth (MLD) with higher irradiance may lead to suppressed bacterial production and a lower bacterial S demand (Simó and

BGD
11, 2267–2303, 2014

Pedrós-Alió, 1999). In these circumstances, bacterial DMSP cleavage may increase in relative importance to the de/de pathway, resulting in higher DMS yields. E01 at Mingulay Reef is a seasonally stratified site which had a relatively shallow MLD of 13 m at the time of sampling, whilst E04 in the southern North Sea is a perennially tidally mixed site with mixing down to the bottom at 33 m. As such the microbial communities at each station may be physiologically adapted to the prevailing conditions, with those at Mingulay experiencing higher levels of oxidative stress in a relatively shallow mixed layer, and thus lower bacterial production. The turbid, mixed water column of the southern North Sea at E04 may induce less irradiance stress on the community, so processes dominate which result in a lower overall potential DMS yield. Thus when the respective communities are exposed to the stress associated with high CO_2, they differ in the sensitivity of their DMS production response. Further investigation is now needed to verify the extent of the influence of phytoplankton community structure and bacterial processes on the sensitivity of surface ocean DMS systems to elevated CO_2, and how the physical and biogeochemical characteristics of different regions may determine this response.

5 Summary and conclusions

We observed that rapid and short term experimental manipulations of CO_2 and $[H^+]$ induced consistent, marked increases in DMS, and decreases in DMSP, in contrast to results from mesocosm experiments. Mesocosms focus on longer timescales (up to 5 weeks) within the framework of a nutrient-induced phytoplankton bloom. This allows a "winners and losers" dynamic, encouraging shifts to species with greater resilience for change. The resultant DMS(P) response reflects the ensuing taxonomic changes (Vogt et al., 2008; Hopkins et al., 2010; Avgoustidi et al., 2012; Archer et al., 2013). The bioassay results we present represent an "acclimatory" response characterised by the lack of ability of small phytoplankton (< 10 µm) to adapt to the altered carbonate chemistry. Stress-induced algal processes (increased cell permeability resulting in in-

BGD
11, 2267–2303, 2014

creased DMSP release and cleavage to DMS and/or direct up-regulation of intracellular DLA and DMS release) likely dominated the response. Rates of DMSP synthesis by algal cells markedly decreased in response to OA in two of the experiments, likely a reflection of a decline in biological productivity. Bacterial processes involved in DMS(P) production and cycling were resilient to OA, and the response varied according to location. Bacterial processes are driven by variations in the physics and biogeochemistry, resulting in sensitivity differences between algal and bacterial communities to increasing CO_2. A similar combination of processes drives seasonal decouplings of DMS and DMSP in the temperate surface ocean, though on much larger spatial and temporal scales (Simó and Pedrós-Alió, 1999; Dacey et al., 1998; Vial-Costa et al., 2008; Archer et al., 2009).

Although it would be inappropriate to extrapolate our small scale, short term results to future DMS sea-to-air fluxes, our study provides further evidence that the DMS system has a capacity to change in the face of future environmental change. Only one modelling study has attempted to quantify the climate response to OA-induced changes to sea surface DMS concentrations (Six et al., 2013). Though an important step forward, the study used model parameterisations based on empirical relationships between DMS and $[H^+]$ from mesocosm studies, and is thus limited by the low level of understanding of the processes behind the observed responses to OA. The variables and rates we report improve our understanding of the sensitivity of the reduced sulphur cycle to future OA, and may contribute to the development of a mechanistic approach to modelling future DMS concentrations (Polimene et al., 2012).

Supplementary material related to this article is available online at http://www.biogeosciences-discuss.net/11/2267/2014/bgd-11-2267-2014-supplement.pdf.

Acknowledgements. This work is a contribution to the UK Ocean Acidification Research Programme (UKOA) which was jointly funded by the Department for Environment, Food and Rural

BGD
11, 2267–2303, 2014

Affairs (Defra), the Natural Environment Research Council (NERC) and the Department for Energy and Climate Change (DECC) under grant agreement no. NE/H017259/1. We are grateful to all members of the scientific party for aiding the success of cruise D366. In particular, we thank Sophie Richier and Mark Moore for the design and management of the experimental bioassays, Toby Tyrell as lead PI of the UKOA Sea Surface Consortium, and Eric Achterberg for leadership as chief scientist. Thanks also to Ross Holland for flow cytometry data, Alex Poulton for primary production data and Michelle Barnett for microscopy counts, Mark Stinchcombe for nutrient data, and Cynthia Dumousseaud for carbonate chemistry measurements. Finally, we thank the captain and the crew of the RSS Discovery, and the technical staff of the National Marine Facilities, for support and assistance during the cruise. We are grateful to Tom Bell for comments that helped to significantly improve the manuscript.

References

Andreae, M. O.: Ocean-atmosphere interactions in the global biogeochemical sulfur cycle, Mar. Chem., 30, 1–29, 2011.

Archer, S. D., Cummings, D. G., Llewellyn, C. A., and Fishwick, J. R.: Phytoplankton taxa, irradiance and nutrient availability determine the seasonal cycle of DMSP in temperate shelf seas, Mar. Ecol.-Prog. Ser., 394, 111–124, 2009.

Archer, S. D., Ragni, M., Webster, R., Airs, R. L., and Geider, R. J.: Dimethyl sulfoniopropionate and dimethyl sulfide production in response to photoinhibition in *Emiliania huxleyi*, Limnol. Oceanogr., 55, 1579–1589, 2010.

Archer, S. D., Tarran, G. A., Stephens, J. A., Butcher, L. J., and Kimmance, S. A.: Combining cell sorting with gas chromatography to determine phytoplankton group-specific intracellular dimethylsulphoniopropionate, Aquat. Microb. Ecol., 62, 109–121, 2011.

Archer, S. D., Kimmance, S. A., Stephens, J. A., Hopkins, F. E., Bellerby, R. G. J., Schulz, K. G., Piontek, J., and Engel, A.: Contrasting responses of DMS and DMSP to ocean acidification in Arctic waters, Biogeosciences, 10, 1893–1908, doi:10.5194/bg-10-1893-2013, 2013.

Arnold, H. E., Kerrison, P., and Steinke, M.: Interacting effects of ocean acidification and warming on growth and DMS-production in the haptophyte coccolithophore *Emiliania huxleyi*, Glob. Change Biol., 19, 1007–1016, doi:10.1111/gcb.12105, 2013.

BGD
11, 2267–2303, 2014

Avgoustidi, V., Nightingale, P. D., Joint, I., Steinke, M., Turner, S. M., Hopkins, F. E., and Liss, P. S.: Decreased marine dimethyl sulfide production under elevated CO_2 levels in mesocosm and in vitro studies, Environ. Chem., 9, 399–404, 2012.

Bailey, K. E., Toole, D., Blomquist, B., Najjar, R. G., Huebert, B., Kieber, D. J., Kiene, R. P., Matrai, P., Westby, G. R., and del Valle, D. A.: Dimethylsulfide production in Sargasso Sea eddies, Deep-Sea Res. Pt. II, 55, 1491–1504, 2008.

Barnes, I., Hjorth, J., and Mihalopoulos, N.: Dimethyl sulfide and dimethyl sulfoxide and their oxidation in the atmosphere, Chem. Rev., 106, 940–975, 2006.

Brussaard, C. P. D., Noordeloos, A. A. M., Witte, H., Collenteur, M. C. J., Schulz, K., Ludwig, A., and Riebesell, U.: Arctic microbial community dynamics influenced by elevated CO_2 levels, Biogeosciences, 10, 719–731, doi:10.5194/bg-10-719-2013, 2013.

Calderia, K. and Wickett, M. E.: Anthropogenic carbon and ocean pH, Nature, 425, 365, doi:10.1038/425365a, 2003.

Caldeira, K. and Wickett, M. E.: Ocean model predictions of chemistry changes from carbon dioxide emissions to the atmosphere and ocean, J. Geophys. Res., 110, C09S04, doi:10.1029/2004JC002671, 2005.

Charlson, R. J., Lovelock, J. E., Andreae, M. O., and Warren, S. G.: Oceanic phytoplankton, atmospheric sulphur, cloud albedo and climate, Nature, 326, 655–661, 1987.

del Valle, D. A., Kieber, D. J., Toole, D. A., Brinkley, J., and Kiene, R. P.: Biological consumption of dimethylsulphide (DMS) and its importance in DMS dynamics in the Ross Sea, Antarctica, Limnol. Oceanogr., 54, 785–798, 2009.

Engel, A., Schulz, K. G., Riebesell, U., Bellerby, R., Delille, B., and Schartau, M.: Effects of CO_2 on particle size distribution and phytoplankton abundance during a mesocosm bloom experiment (PeECE II), Biogeosciences, 5, 509–521, doi:10.5194/bg-5-509-2008, 2008.

Engel, A., Borchard, C., Piontek, J., Schulz, K. G., Riebesell, U., and Bellerby, R.: CO_2 increases $_{14}C$ primary production in an Arctic plankton community, Biogeosciences, 10, 1291–1308, doi:10.5194/bg-10-1291-2013, 2013.

Flynn, K. J., Blackford, J. C., Baird, M. E., Raven, J. A., Clark, D. R., Beardall, J., Brownlee, C., Fabian, H., and Wheeler, G. L.: Changes in pH at the exterior surface of plankton with ocean acidification, Nature Clim. Change, 2, 510–513, 2012.

Gabric, A. J., Matrai, P. A., and Vernet, M.: Modelling the production and cycling of dimethylsulphide during the vernal bloom in the Barents Sea, Tellus B, 51, 919–937, 1999.

BGD
11, 2267–2303, 2014

Galí, M., Ruiz-González, Lefort, T., Gasol, J. M., Cardelús, C., Romera-Castillo, C., and Simó, R.: Spectral irradiance dependence of sunlight effects on plankton dimethylsulphide production, Limnol. Oceanogr., 58, 489–504, 2013.
Hendriks, I. E., Duarte, C. M., and Álvarez, M.: Vulnerability of marine biodiversity to ocean acidification: a meta-analysis, Estuar. Coast. Shelf S., 86, 157–164, 2010.
Hönisch, B., Ridgwell, A., Schmidt, D. N., Thomas, E., Gibbs, S.J., Sluijs, A., Zeebe, R., Kump, L., Martindale, R. C., Greene, S. E., Kiessling, W., Ries, J., Zachos, J. C., Royer, D. L., Barker, S., Marchitto Jr., T. M., Moyer, R., Pelejero, C., Ziveri, P., Foster, G. L., and Williams, B.: The geological record of ocean acidification, Science, 335, 1058–1063, 2012.
Hopkins, F. E., Turner, S. M., Nightingale, P. D., Steinke, M., and Liss, P. S.: Ocean acidification and marine biogenic trace gas production, P. Natl. Acad. Sci. USA, 107, 760–765, 2010.
Kiene, R. P. and Slezak, D.: Low dissolved DMSP concentrations in seawater revealed by small-volume gravity filtration and dialysis sampling, Limnol. Oceanogr.-Meth., 4, 80–95, 2006.
Kiene, R. P., Linn, L. J., and Bruton, J. A.: New and important roles for DMSP in marine microbial communities, J. Sea Res., 43, 209–224, 2000.
Kiene, R. P., Kieber, D. J., Slezak, D., Toole, D. A., del Valle, D. A., Bisgrove, J., Brinkley, J., and Rellinger, A.: Distribution and cycling of dimethylsulphide, dimethylsulfoniopropionate, and dimethylsulfoxide during spring and early summer in the Southern Ocean south of New Zealand, Aquat. Sci., 69, 305–319, 2007.
Kim, J.-M., Lee, K., Yang, E. J., Shin, K., Noh, J. H., Park, K.-T., Hyun, B., Jeong, H.-J., Kim, J.-H., Kim, K. Y., Kim, M., Kim, H.-C., Jang, P.-G., and Jang, M.-C.: Enhanced production of oceanic dimethylsulphide resulting from CO_2-induced grazing activity in a high CO_2 world, Environ. Sci. Technol., 44, 8140–8143, 2010.
Lana, A., Bell, T. G., Simó, R., Vallina, S. M., Ballabrera-Poy, J., Kettle, A.-J., Dachs, J., Bopp, L., Saltzman, E. S., Stefels, J., Johnson, J. E., and Liss, P. S.: An updated climatology of surface ocean dimethylsulphide concentrations and emission fluxes in the global ocean, Global Biogeochem. Cy., 25, GB1004, doi:10.1029/2010GB003850, 2011.
Liu, J., Weinbauer, M. G., Maier, C., Dai, M., and Gattuso, J.-P.: Effect of ocean acidification on microbial diversity and on microbe-driven biogeochemistry and ecosystem functioning, Aquat. Microb. Ecol., 61, 291–305, 2010.
Marie, D., Brussaard, C. P. D., Partensky, F., and Vaulot, D.: Enumeration of phytoplankton, bacteria and viruses in marine samples, in: Current Protocols in Cytometry, edited by: Robin-

BGD
11, 2267–2303, 2014

son, J. P., Darzynkiewicz, Z., Dean, P. N., Rabinovitch, P. S., Stewart, C. C., Tanke, H. J., and Wheeless, L. L., John Wiley and Sons, 11.11.11–11.11.15, 1999.
Meakin, N. G. and Wyman, M.: Rapid shifts in picoeukaryote community structure in response to ocean acidification, ISME J., 5, 1397–1405, 2011.
Miles, C. J., Bell, T. G., and Suntharalingam, P.: Investigating the inter-relationships between water attenuated irradiance, primary production and DMS(P), Biogeochemistry, 110, 201–213, 2012.
Moran, M. A., Reisch, C. R., Kiene, R. P., and Whitman, W. B.: Genomic insights into bacterial DMSP transformations, Annu. Rev. Mar. Sci., 4, 523–542, 2012.
Newbold, L. K., Oliver, A. E., Booth, T., Tiwari, B., DeSantis, T., Maguire, M., Andersen, G., van der Gast, C. J., and Whiteley, A. S.: The response of marine picoplankton to ocean acidification, Environ. Microbiol., 14, 2293–2307, 2012.
Piontek, J., Borchard, C., Sperling, M., Schulz, K. G., Riebesell, U., and Engel, A.: Response of bacterioplankton activity in an Arctic fjord system to elevated pCO_2: results from a mesocosm perturbation study, Biogeosciences, 10, 297–314, doi:10.5194/bg-10-297-2013, 2013.
Polimene, L., Archer, S. D., Butenschön, M., and Allen, J. I.: A mechanistic explanation for the Sargassa Sea DMS "summer paradox", Biogeochemistry, 110, 243–255, 2012.
Rap, A., Scott, C. E., Spracklen, D. V., Bellouin, N., Forster, P. M., Carslaw, K. C., Schmidt, A., and Mann, G.: Natural aerosol direct and indirect radiative effects, Geophys. Res. Lett., 40, 3297–3301, 2013.
Raven, J. A., Caldeira, K., Elderfield, H. E., Hoegh-Guldberg, O., Liss, P. S., Riebesell, U., Shepherd, J., Turley, C., and Watson, A.: Ocean Acidification due to Increasing Atmospheric Carbon Dioxide, Royal Society, London, UK, 2005.
Rees, A. P., Joint, I., and Donald., K. M.: Early spring bloom phytoplankton-nutrient dynamics at the Celtic Sea Shelf Edge, Deep-Sea Res. Pt. I, 46, 483–510, 1999.
Richier, S., Achterberg, E. P., Dumousseaud, C., Poulton, A. J., Suggett, D. J., Tyrell, T., and Moore, C. M.: Carbon cycling and phytoplankton responses within highly-replicated shipboard carbonate manipulation experiments around the Northwest European continental shelf, Biogeosciences Discuss., this issue, 2014.
Riebesell, U. and Tortell, P. D.: Effects of ocean acidification on pelagic organisms and ecosystems, in: Ocean Acidification, edited by: Gattuso, J.-P. and Hansson, L., Oxford University Press, 99–121, 2011.

BGD
11, 2267–2303, 2014

Simó, R.: From cells to globe: approaching the dynamics of DMS(P) in the ocean at multiple scales, Can. J. Fish. Aquat. Sci., 61, 673–684, 2004.
Simó, R. and Pedrós-Alió, C.: The role of vertical mixing in controlling the oceanic production of dimethyl sulphide, Nature, 402, 396–399, 1999.
Simó, R., Pedrós-Alió, C., Malin, G., and Grimalt, J. O.: Biological turnover of DMS, DMSP and DMSO in contrasting open-sea waters, Mar. Ecol.-Prog. Ser., 203, 1–11, 2000.
Simó, R., Archer, S. D., Pedrós-Alió, C., Gilpin, L., and Stelfox-Widdicombe, C. E.: Coupled dynamics of dimethylsulfoniopropionate and dimethylsulphide cycling and the microbial food web in surface waters of the North Atlantic, Limnol. Oceanogr., 47, 53–61, 2002.
Six, K. D., Kloster, S., Ilyina, T., Archer, S. D., and Zhang, K.: Global warming amplified by reduced sulphur fluxes as a result of ocean acidification, Nature Clim. Change, 3, 975–978, 2013.
Spielmeyer, A. and Pohnert, G.: Influence of temperature and elevated carbon dioxide on the production of dimethylsulfoniopropionate and glycine betaine by marine phytoplankton, Mar. Environ. Res., 73, 62–69, 2012.
Stefels, J.: Physiological aspects of the production and conversion of DMSP in marine algae and higher plants, J. Sea Res., 43, 183–197, 2000.
Stefels, J., Steinke, M., Turner, S., Malin, G., and Belviso, S.: Environmental constraints on the production and removal of the climatically active gas dimethylsulphide (DMS) and implications for ecosystem modelling, Biogeochemistry, 83, 245–275, 2007.
Stefels, J., Dacey, J. W. H., and Elzenga, T. M.: In vivo DMSP-biosynthesis measurements using stable-isotope incorporation and proton-transfer-reaction mass spectrometry (PTR-MS), Limnol. Oceanogr.-Meth., 7, 595–611, 2009.
Sunda, W., Kieber, D. J., Kiene, R. P., and Huntsman, S.: An antioxidant function for DMSP and DMS in marine algae, Nature, 418, 317–320, 2002.
Sunda, W. G., Hardison, R., Kiene, R. P., Bucciarelli, E., and Harada, H.: The effect of nitrogen limitation on cellular DMSP and DMS release in marine phytoplankton: climate feedback implications, Aquat. Sci., 69, 341–351, 2007.
Toole, D. A. and Siegel, D. A.: Light-driven cycling of dimethylsulphide (DMS) in the Sargasso Sea: closing the loop, Geophys. Res. Lett., 31, L09308, doi:10.1029/2004GL019581, 2004.
Toole, D. A., Kieber, D. J., Kiene, R. P., Siegel, D. A., and Nelson, N. B.: Photolysis and the dimethylsulfide (DMS) summer paradox in the Sargasso Sea, Limnol. Oceanogr., 48, 1088–1100, 2003.

BGD
11, 2267–2303, 2014

Toole, D. A., Slezak, D., Kiene, R. P., Kieber, D. J., and Siegel, D. A.: Effects of solar radiation on dimethylsulphide cycling in the western Atlantic Ocean, Deep-Sea Res. Pt. I, 53, 136–153, 2006.

Vallina, S. M. and Simó, R.: Strong relationship between DMS and the solar radiation dose over the global surface ocean, Science, 315, 506–508, 2007.

Vila-Costa, M., Kiene, R. P., and Simó, R.: Seasonal variability of the dynamics of dimethylated sulfur compounds in a coastal northwest Mediterranean site, Limnol. Oceanogr., 53, 198–211, 2008.

Vogt, M., Steinke, M., Turner, S., Paulino, A., Meyerhöfer, M., Riebesell, U., LeQuéré, C., and Liss, P.: Dynamics of dimethylsulphoniopropionate and dimethylsulphide under different CO_2 concentrations during a mesocosm experiment, Biogeosciences, 5, 407–419, doi:10.5194/bg-5-407-2008, 2008.

Weinbauer, M. G., Mari, X., and Gattuso, J.-P.: Effect of ocean acidification on the diversity and activity of heterotrophic marine microorganisms, in: Ocean Acidification, edited by: Gattuso, J.-P. and Hansson, L., Oxford University Press, 99–121, 2011.

Wingenter, O. W., Haase, K. B., Zeigler, M., Blake, D. R., Rowland, F. S., Sive, B. C., Paulino, A., Runar, T., Larsen, A., Schulz, K., Meyerhofer, M., and Riebesell, U.: Unexpected consequences of increasing CO_2 and ocean acidity on marine production of DMS and CH_2ClI: potential climate impacts, Geophys. Res. Lett., 34, L05710, doi:10.1029/2006GL028139, 2007.

Wolfe, G. V., Levasseur, M., Cantin, G., and Michaud, S.: Microbial consumption and production of dimethyl sulfide (DMS) in the Labrador Sea, Aquat. Microb. Ecol., 18, 197–205, 1999.

Zubkov, M. V., Fuchs, B. M., Archer, S. D., Kiene, R. P., Amann, R., and Burkhill, P. H.: Rapid turnover of dissolved DMS and DMSP by defined bacterioplankton communities in the stratified euphotic zone of the North Sea, Deep-Sea Res. Pt. II, 49, 3017–3038, 2002

Zubkov, M., Linn, L. J., Amann, R., and Kiene, R. P.: Temporal patterns of biological dimethylsulphide (DMS) consumption during laboratory-induced phytoplankton bloom cycles, Mar. Ecol.-Prog. Ser., 271, 77–86, 2004.

BGD
11, 2267–2303, 2014

Table 1. Overview of initial conditions for experimental bioassays. MLD = mixed layer depth, TON: total organic nitrogen, Si: silicate, P: phosphate, DMSPt = total DMSP, $DMSP_p$ = particulate DMSP. Data shown are means (±standard error) for triplicate measurements made at 0 h for each experiment. Standard errors are not shown for experimental pCO_2 and pH as values are based on single measurements.

	E01 56°47.688′ N 7°24.300′ W Mingulay Reef 8 Jun 2011	E02 52°28.237′ N 5°54.052′ W Irish Sea 14 Jun 2011	E03 46°12.137′ N 7°13.253′ W Bay of Biscay 21 Jun 2011	E04 52°59.661′ N 2°29.841′ E S North Sea 26 Jun 2011	E05 56°30.293′ N 3°39.506′ E Mid North Sea 2 Jul 2011
Regime	Stratified	Mixed	Stratified	Mixed	Stratified
Sample depth (m)	6	5	10	5	12
MLD (total depth) (m)	13 (190)	76 (76)	44 (4760)	33 (33)	14 (72)
T (°C)	11.3	11.8	15.3	14.6	14.0
Salinity	34.8	34.4	35.8	34.1	35.0
pCO_2 (µatm)					
in situ	342.6 ± 2.4	333.7 ± 3.1	339.8 ± 3.5	400.6 ± 3.3	368.1 ± 2.5
Ambient	342.3	no data	345.4	395.4	374.7
~ 550	564.1	533.4	531.2	533.4	528.9
~ 750	746.4	no data	674.0	691.4	730.5
~ 1000	969.6	862.7	877.8	936.6	917.5
pH					
in situ	8.11 ± 0.003	8.11 ± 0.004	8.12 ± 0.004	8.05 ± 0.003	8.07 ± 0.003
Ambient	8.10	no data	8.10	8.05	8.07
~ 550	7.91	7.94	7.95	7.94	7.94
~ 750	7.80	no data	7.85	7.84	7.82
~ 1000	7.70	7.75	7.75	7.72	7.73
Nutrients and chl *a*					
TON (µM)	1.1 ± 0.08	0.3 ± 0.003	0.6 ± 0.0	0.9 ± 0.08	0.3 ± 0.10
Si (µM)	2.1 ± 0.14	0.5 ± 0.003	0.6 ± 0.004	0.8 ± 0.0	0.1 ± 0.01
P (µM)	0.1 ± 0.02	0.1 ± 0.007	0.1 ± 0.004	0.1 ± 0.007	0.1 ± 0.018
Total chl *a* (µg L^{-1})	3.3 ± 0.04	3.5 ± 0.07	0.8 ± 0.04	1.3 ± 0.03	0.3 ± 0.01
> 10 µm chl *a* (µg L^{-1})	no data	2.8 ± 0.12	0.3 ± 0.02	0.3 ± 0.03	0.1 ± 0.002
DMS parameters					
DMSPt (nmol L^{-1})	59.6 ± 0.7	25.9 ± 1.9	44.6 ± 1.3	8.0 ± 0.4	15.1 ± 0.5
DMS (nmol L^{-1})	1.1 ± 0.02	0.7 ± 0.02	2.1 ± 0.2	1.1 ± 0.02	1.3 ± 0.1
DMSPt : chl *a* (nmol µg $^{-1}$)	18.3 ± 0.2	9.2 ± 0.2	58.1 ± 3.8	6.2 ± 0.3	61.1 ± 3.4
DMS : *DMSPt*	0.02 ± 0.001	0.03 ± 0.002	0.05 ± 0.004	0.14 ± 0.004	0.09 ± 0.002

BGD
11, 2267–2303, 2014

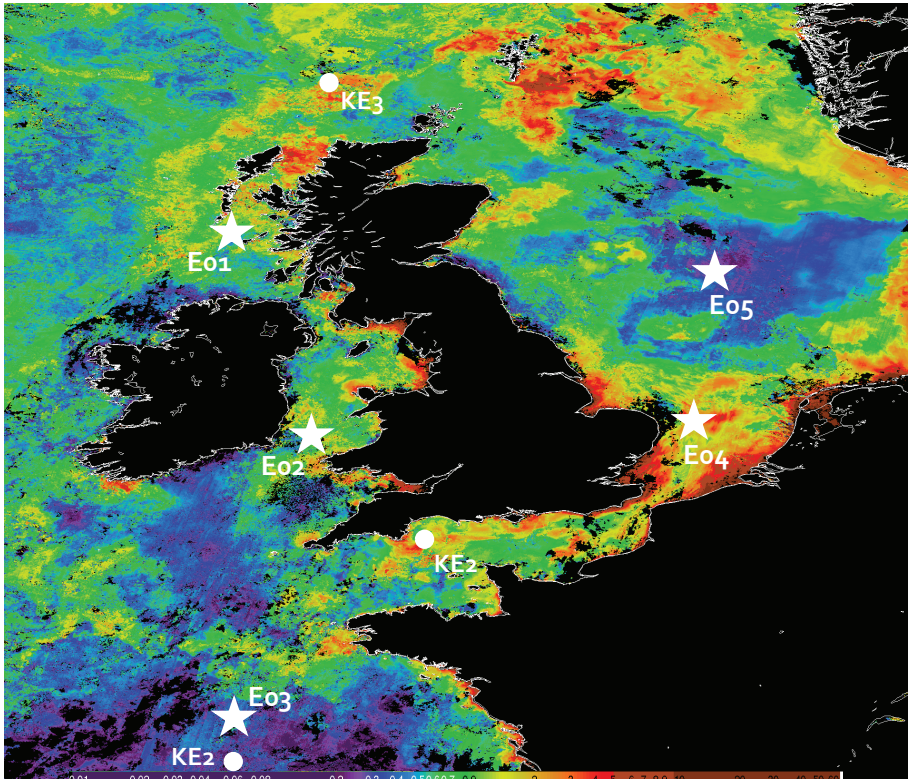

Fig. 1. Locations of sampling in NW European shelf waters for bioassay experiments (white stars, E01–E05) and for kinetic experiments (white circles, KE1–KE3). Map shows MERIS chlorophyll composite for period 6–12 June 2011 as a representative week of the sampling period (8 June–5 July 2011). Satellite image courtesy NEODAAS.

BGD
11, 2267–2303, 2014

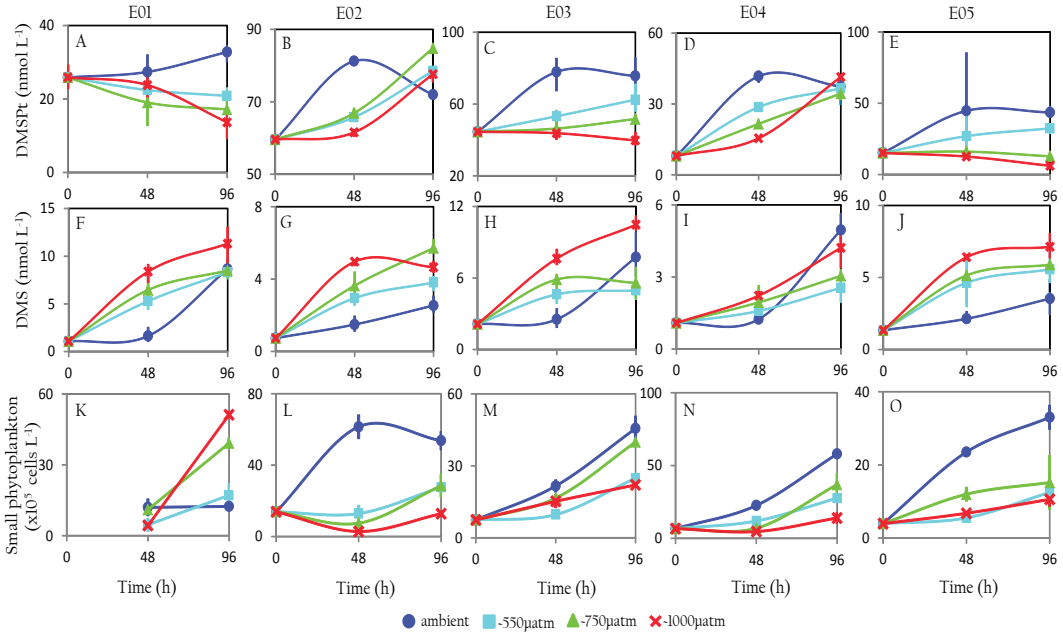

Fig. 2. Concentrations (nmol L^{-1}) of total DMSP **(A–E)** and DMS **(F–J)** during five bioassay experiments, and abundance of total small phytoplankton (< 10 µm) **(K–O)** (×10^5 cells L^{-1}). See Table 2 for specific pCO_2 and pH for each experiment. Values shown are means of experimental triplicates, and error bars indicate the standard error. Different scales are used on plots to ensure trends are visible.

BGD
11, 2267–2303, 2014

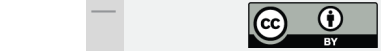

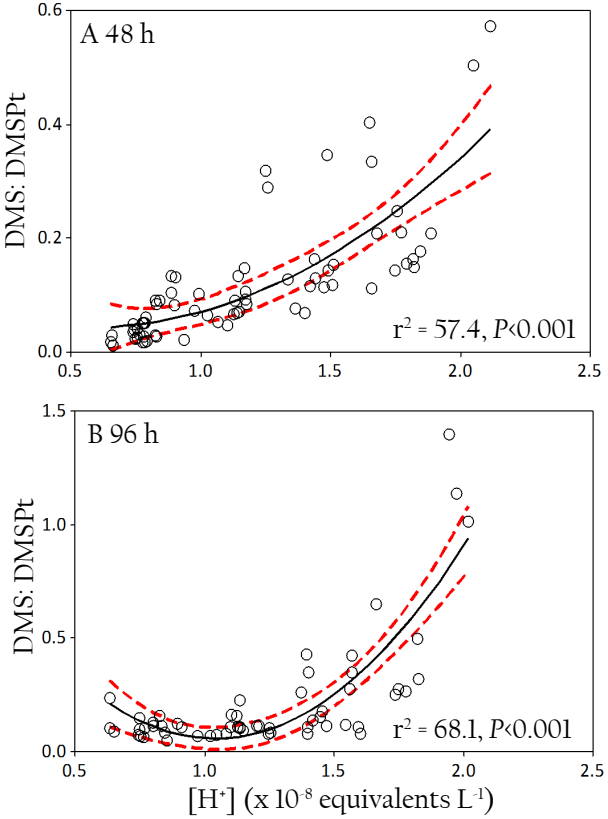

Fig. 3. Relationship between DMS : *DMSPt* and H^+ concentration, ($[H^+] \times 10^{-8}$ equivalents L^{-1}) at 48 h **(A)** and 96 h **(B)** for all data from all five bioassay experiments. Black line indicates regression fit to data, and red dashed lines indicate the 95 % confidence intervals for the relationship. Coefficients of determination (r^2) and the significance of the *F* ratio of *ANOVA* of the regression are shown (n = 60).

BGD
11, 2267–2303, 2014

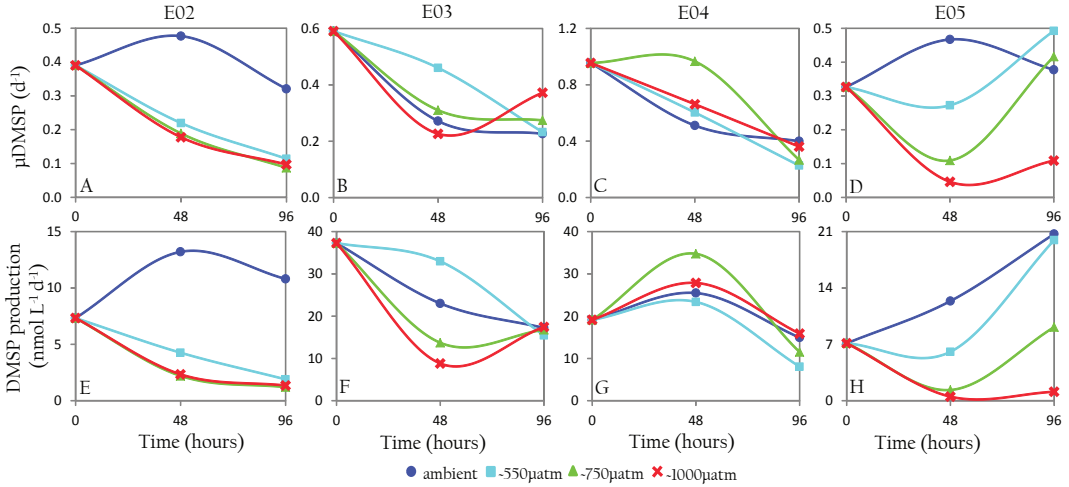

Fig. 4. De novo synthesis (d^{-1}) of DMSP **(A–D)** and DMSP production rates ($nmol\,L^{-1}\,d^{-1}$) **(E–H)** for E02–E05 (data not available for E01).

BGD
11, 2267–2303, 2014

Consistent increase in DMS in response to high CO_2

F. E. Hopkins and S. D. Archer

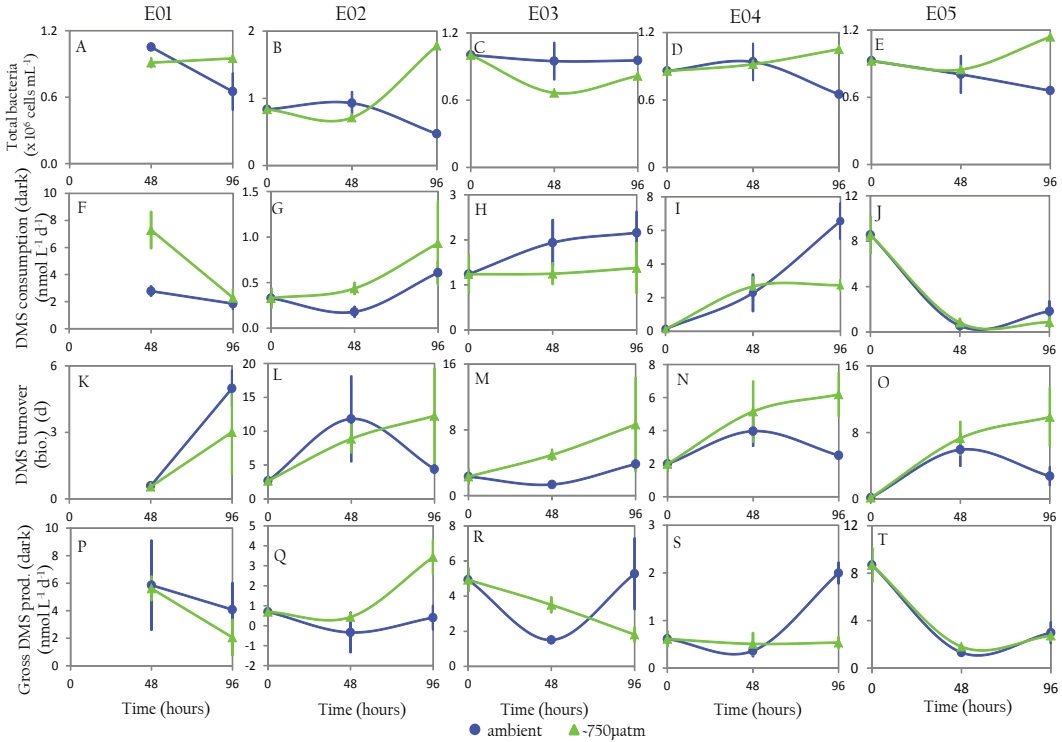

Fig. 5. DMS consumption rates (nmol L^{-1} d^{-1}) **(A–E)**, biological DMS turnover (d) **(F–J)**, DMS gross production rates **(K–O)**, and total bacteria counts (cells mL^{-1}) **(P–T)** during five bioassay experiments at ambient pCO_2 and ~ 750µatm. DMS turnover times (d) = 1/loss rate constant (k_{BC},d^{-1}). Data is summarised in Table 6. Error bars indicate standard error on triplicate rate measurements. Asterisks (*) denote significant difference from ambient bioassays (Significance of F ratio from ANOVA, $p < 0.05$). No measurements were made at 0 h for E01.

BGD
11, 2267–2303, 2014

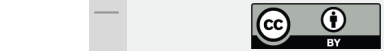

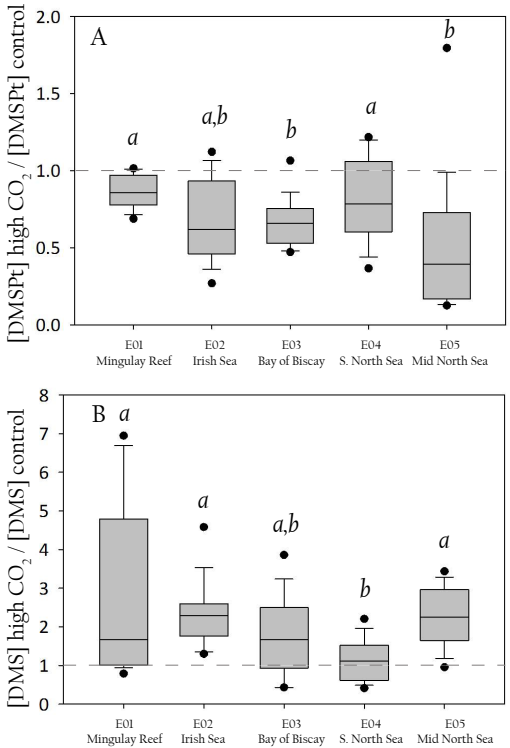

Fig. 6. Box plots summarising relative differences ([*x*] high CO_2/[*x*] control) in **(A)**: DMSPt and **(B)**: DMS between ambient control and high CO_2 treatments for each experimental bioassay (all data from all time points). Plots show interquartile range (box), median values (horizontal line in box), mean values (open circles), range of data (error bars) and outliers (closed circles, outside 1.5× interquartile range). Italicised letters (*a*, *b*) indicate statistical groupings derived from one-way ANOVA and pairwise comparisons (Tukey's/Dunn's, significant differences between pairs if $P < 0.05$). Grey dashed line indicates a value of 1 = no difference between ambient controls and high CO_2 treatments.

BGD
11, 2267–2303, 2014